

# Assessment of potential beach erosion risk and impact of coastal zone development: a case study on Bongpo-Cheonjin Beach

Changbin Lim<sup>1</sup>, Taekon Kim<sup>1</sup>, Sahong Lee<sup>1</sup>, Yoon Jeong Yeon<sup>1</sup>, Jung Lyul Lee<sup>1,2</sup>

<sup>1</sup>School of Civil, Architecture and Environmental System Engineering, Sungkyunkwan University, Suwon 16419, Republic of Korea

<sup>2</sup>Graduate School of Water Resources, Sungkyunkwan University, Suwon 16419, Republic of Korea

Corresponding author: Jung Lyul Lee ([jillee6359@hanmail.net](mailto:jillee6359@hanmail.net))

## Abstract

Coastal erosion is much severe due to human-induced coastal zone development and storm impact, in addition to climate change. In this study, the beach erosion risk is defined, followed by a quantitative assessment of potential beach erosion risk based on three components associated with watershed, coastal zone development and episodic storm, respectively. On an embayed beach, the background erosion due to development in a watershed affects sediment supply from a river to the beach, while alongshore redistribution of sediment transport caused by construction of harbor induces shoreline reshaping, for which the equilibrium bay shape model of parabolic type is adopted. To evaluate the beach erosion during storm, the return period (frequency) of a storm occurrence is evaluated from long-term beach survey data conducted four times per year. Beach erosion risk is defined and assessment is carried out for each component, from which the results are combined to construct a combined potential erosion risk curve to be used in the environmental impact assessment. Finally, the proposed method is applied to Bongpo-Cheonjin Beach in Gangwon-do, Korea, with the support of a series of aerial photographs taken from 1972 to 2017 and beach survey data commenced since 2010. The satisfactory outcome derived from this study are expected to benefit eroding beaches elsewhere.

*Key words: Beach erosion risk, Quantitative assessment, Parabolic model, Storm impact, Combined potential erosion risk curve.*

## 1 Introduction

In recent years, erosion of sandy beaches has worsened in many countries due to development in the watershed and coastal zone, construction of artificial structures, storm impact, and climate change. Among these factors, the scale of coastal zone development has threatened beach safety arising from (1) reduction of upstream sediment supply, (2) changes in nearshore wave fields following the installation of harbor structures, (3) inappropriate large-scale reclamation without preventive measures, and (4) decrease in beach width due to forest plantation and construction of roads and infrastructures.

Coastal erosion is often accompanied by environmental and social problems. In many developed countries, including Korea, coastal environments are deteriorated and beach narrowed due to urbanization. However, because it is difficult to accurately quantify the cause of erosion and logically infer the mechanism, it does not fundamentally alleviate the motive, but over protects the eroding coast, causing another problem or wasting public investments. Therefore, it is imperative to evaluate the existing regulations for beach erosion control and guidelines for coastal development, as well as to incorporate environmental impact assessment into a comprehensive licensing system. To achieve these goals, an appropriate method is required to assess the risk of beach erosion and determine the most effective strategy.

In general, beach erosion may be caused by the decrease of sediment to a beach, by shoreline reshaping within a littoral cell due to construction of large structures, and by bar formation during storm. Because sedimentation problems on a sandy coast is a multi-scale spatiotemporal process associated with different mechanisms, and shoreline planform is constantly evolving (Stive et al., 2002, 2009; Miller and Dean, 2004), it is not only difficult to find publication that includes all these mechanisms, but also hard to discover good cases where the cause of erosion is identified in various time and space scales. However, Toimil et al. (2017) have simplified the shoreline migration by disassociating long-shore processes (e.g., Zacharioudaki and Reeve, 2011; Casas Prat and Sierra, 2012), which are mostly responsible for long-term changes, from those induced in cross-shore direction (e.g., Callaghan et al., 2008; Wainwright et al., 2015) which tend to produce changes in the short-term and over seasonal time scales. In addition, Ballesteros et al. (2018) have classified the main factors inducing coastal erosion into three components, long-term (associated with a timescale of several decades), medium-term (associated with a timescale from years to few decades) and episodic terms (associated with a timescale from days to months), on the basis of different processes acting at different timescales.

A beach can retain stability when sediment budget is balanced within a closed littoral cell, such as in an embayed beach. Therefore, it is essential to analyze sediment transport in both alongshore and cross-shore directions (e.g., Inman and Jenkins, 1984; Bray et al., 1995). When the amount of sediment entering or leaving a littoral cell changes, a new equilibrium volume of sediment is established within the cell accordingly (Dolan et al., 1987; Kana and Stevens, 1992; Pethick, 1996; Cooper, 1997; Cooper and Pethick, 2005). On the other hand, the amount of sediment supplied from a river and that lost into the open sea due to the continuous wave action should also be regarded as main components in the sediment budget. For example, a decrease in sediment discharge due to the construction of dams (Foley et al., 2017; Warrick et al., 2019) or an increase in sediment loss due to sand mining (Edward et al., 2006) has caused gradual shoreline retreat. In addition, Lee and Lee (2020) have recently proposed an equation to calculate the beach width according to the law of mass conservation by placing variables to represent the main factors in sediment budget.

It is well known that wave diffraction and change in longshore sediment transport direction occurs downdrift of a harbor where shoreline reshaping begins, resulting in updrift accretion and downdrift erosion. Numerous observations and studies have been conducted to assess/predict longshore sediment transport rate in a wave-sediment environment (Komar and Inman, 1970; CERC, 1984; Kamphuis, 2002; Bayram et al., 2007). Empirical models have been used to estimate the equilibrium shoreline in the areas affected by harbor breakwater. Among them, the parabolic bay shape equation (PBSE; Hsu and Evans, 1989) for

65 headland-bay beaches in static equilibrium has been recognized for its practicality in many countries and has been used for coastal management (USACE, 2002; Herrington et al., 2007; Bowman et al., 2009; González et al., 2010; Silveira et al., 2010; Yu and Chen, 2011; Anh et al., 2015; Thomas et al., 2016; Ab Razak et al., 2018a & 2018b). Recently, Lim et al. (2021) have extended the parabolic model (Hsu and Evans, 1989) to beaches in polar coordinates and prove the versatility of this model for embayed beaches.

70 Lastly, cross-shore sediment transport causes morphological changes in beach profile due to high/storm waves, resulting in shoreline retreat. Much work has been done to interpret geomorphological phenomena (Swart, 1974; Wang et al., 1975; Wright et al., 1985; Miler and Dean, 2004; Yates et al., 2009; Montañó et al., 2020). Recently, Kim (2021) proposes a method to estimate the erosion width by the frequency of high waves using statistical analysis of GPS shoreline observation data collected seasonally for more than 10 years. He also devises the concept of horizontal movement of suspended sediments and applies a wave scenario model to analyze the response relationship between the convergent MSL of Yates et al (2009).

The aim of this study is to propose a combined potential erosion risk curve (CPERC) curve for a beach from accumulating the potential risk of three different erosion components (Sect. 3), using a minimum set of field data (e.g., aerial photographs and shoreline survey data). The methodology is then applied to Bongpo-Cheonjin Beach in Korea, as part of environmental impact assessment for planning coastal protection measures.

80 This paper starts with a general introduction in Sect. 1, following by the definition of potential erosion risk and the concept of combined potential erosion risk curve (CPERC) in Sect. 2. Section 3 explains methods for assessing three different erosion factors: (1) sediment input from watershed, (2) construction of harbor breakwater, and (3) storm impact. The methodology is then applied to Bongpo-Cheonjin Beach in Korea, a shallow embayment with high risk of erosion, supported by aerial photographs taken between 1972 and 2017, 37 sets of seasonal shoreline survey data collected during 2008–2017 and NOAA’s wave data, shown in tables and graphs in Sect. 4. Discussions are then given in Sect. 5 for improving the accuracy when applying the method proposed in this study to a different coastal environment. Finally, concluding remarks are made in Sect. 6. It is expected that this quantitative method for the assessment of beach erosion risk will benefit eroding beaches elsewhere in developing and developed countries.

## 2. Beach Erosion Risk

90 Recently, research in coastal impact caused by extreme events, such as hurricanes, has increased in several countries including the United States and Europe, (e.g., Beven II et al., 2008; Kunz et al., 2013; Van Verseveld et al., 2015; Spencer et al., 2015). Among these, Ballesteros et al. (2018) have proposed a methodology, framed within the Source–Pathway–Receptor–Consequence model (SPRC) that will enable the identification of the main factors inducing coastal erosion at different timescales and their associated impact to the beaches on Mediterranean coast. Toimil et al. (2017) have conducted the probabilistic estimate of shoreline retreat for quantifying risk consequences due to climate change on a regional scale. Sanuy et al. (2018) have also established an erosion risk assessment method based on a Bayesian network, and obtained a method to

reduce erosion by applying it to beaches in the Mediterranean. In addition, many studies have been conducted to evaluate coastal risks through analysis and prediction of various physical phenomena and effects using numerical models (e.g., Roelvink et al., 2009; McCall et al., 2010; Harley et al., 2011; Roelvink and Reniers, 2012).

100 However, most risk assessment methods are not only focused on extreme events, but also require numerous data and techniques. Therefore, it may be impractical for coastal managers to apply these methods to field condition for coastal erosion management. In this study, we present a method to assess the potential erosion risk induced by the combined action of processes acting at different time scales and with minimal basic survey data.

## 2.1 Definition of beach erosion risk

105 Many different definitions on risk have been proposed (Knight, 1921; Rasmussen et. al., 1975; Kaplan and Garrick, 1981; Hansson, 2007; Hubbard, 2009). In technical contexts, the word “risk” has several specialized uses and meanings. Among them, risk is defined as the expected loss of the event implying the product of the probability of some event and the loss of the event. It is the standard technical meaning of the term “risk” in many disciplines and it is also regarded by some risk analysts as the only correct usage of the term (Hansson, 2007). In the same context, risk is usually assessed by the time-averaged amount of damage, and its evaluation is possible through time domain, frequency domain, and probability domain analysis. In frequency domain, potential risk  $R$  is defined as the product of consequence (i.e., factor or mechanism)  $C$  and frequency  $F$  such as,

$$R = CF \quad (1)$$

115 In this study,  $R$  is the beach area likely to be damaged by erosion due to development in watershed, on land, and in coastal water. The frequency  $F$  on the right-hand-side of Eq. (1) corresponds to the frequency of erosion risk from the equilibrium shoreline to the landward erosion limit. Where several erosion causes (factor) exist, total erosion risk is taken as the sum of the risk from each contributing factor.

## 2.2 Potential beach erosion risk

The consequence  $C$  in Eq. (1) is obtained from analyzing all the factors affecting the eroded beach surface area. As mentioned in the introduction, coastal erosion is caused by the imbalance in sediment budget, construction of harbor breakwater, and storm impact on the shore. As such, the physical process that causes erosion is characteristically subdivided, so the erosion consequence  $C$  is calculated from the sum of the independently assessed beach erosion area defined as the Potential Erosion Area (PEA) and the Potential Erosion Width (PEW). The former consists of the beach surface area reduced by (1) background erosion due to reduction in sediment input from river called Potential Background Erosion Area (PBEA,  $A_b$ ), (2) alongshore shoreline reshaping due to harbor construction called Potential Reshaping Erosion Area (PREA,  $A_r$ ), and (3) retreat by episodic storm impact called Potential Episodic Erosion Area (PEEA,  $A_e$ ). The latter contains three components called the Potential Background Erosion Width (PBEW,  $W_b$ ), the Potential Reshaping Erosion Width (PREW,  $W_r$ ), and the Potential

130 **Episodic Erosion Width (PEEW,  $W_e$ )**, respectively, which are obtained from dividing each PEA component by effective beach length. In the above, the width of erosion risk is measured shoreward with respect to the **Equilibrium Original ShoreLine (EOSL)**, which can be obtained by a long-term average value prior to the erosion due to coastal zone development.

Since the sediment budget is expressed in volumetric units, information on the vertical dimension of active beaches, defined as the sum of closure depth and berm height, is required to convert to area unit of beach surface. **When a change in the total surface area of a beach in the littoral cell occurs, it is necessary to assess the PBEA and PREA whether it is due to development in a watershed or coastal zone. If there is no change in the total beach surface area within a littoral cell, but the equilibrium shoreline is reshaped and irreversible erosion occurs, assessment of PREA is required. Finally, assessment of the PEEA corresponding to recoverable episodic erosion is required. For the first two erosion factors, the concept of frequency is not required as beach erosion is irrecoverable, but for the third factor, the return frequency (period) of storm occurrence should be considered because wave heights and periods vary with the strength of the storm.**

Each component in the PEA is a term that has units of area and is defined as the potential beach erosion area. Similarly, this definition gives the erosion width for all three component factors as follows,

$$W_b = \frac{A_b}{L_b}, \quad W_r = \frac{A_r}{L_r}, \quad \text{and} \quad W_e = \frac{A_e}{L_e} \quad (2)$$

where  $A_b$ ,  $A_r$ ,  $A_e$ ,  $W_b$ ,  $W_r$  and  $W_e$  correspond to the PBEA, PREA, PEEA, PBEW, PREW and PEEW, respectively, as defined above, and  $L_b$ ,  $L_r$  and  $L_e$  are the effective beach lengths for PBEA, PREA, and PEEA, respectively. The PBEA can be assumed to have a uniform effect along the coast, and for convenience, it is assumed that the same erosion occurs along a coast due to storm impact, so  $L_b$  and  $L_e$  are equal to the length of the beach  $L$ . However, erosion due to shoreline reshaping occurs only in the erosion/accretion zone, so it is less than the beach length  $L$ .

### 2.3 Combined potential erosion risk curve

150 Prior to delimiting the landward boundary of an ideal combined potential erosion risk for a sandy beach, which is the sum of all potential erosion widths from the contributing components, the existing beach status must be clarified. For example, a beach may include a wide buffer zone in which no damage occurs, such as the back beach and dunes that will only be damaged by a storm for a specific number of years, and beach profile can recover after storm wanes; or if the extent of erosion is too large, existing property and infrastructures may be damaged. The extent of current beach width and area on which protection is required must be thoroughly investigated.

For practical application, a **combined potential erosion risk curve (CPERC)** can be constructed by plotting the consequence  $C$  (e.g., combined potential erosion risk area) versus combined potential erosion width, with respect to the shoreward distance from the average shoreline (i.e., EOSL). By expressing the EOSL in polar coordinates, and if the circle that best fits the current average shoreline is obtained, the center of the circle  $O$  can be determined. As shown in Fig. 1, the average shoreline is located at  $R_o$  from the reference pole, the beach landward limit (red dashed line in Fig. 1) is located at  $R_{ec}$  from the origin, and each angle  $\alpha$  has different values depending on its boundary configuration. Therefore, if  $R_o$  and  $R_{ec}$  are determined for each angle

160  $\alpha$ , a **combined potential erosion risk curve (CPERC)** is obtained by an appropriate equation according to the shoreward distance  $r$  from the EOSL, such as,

$$C(r) = \int_{\alpha=0}^{\alpha=\alpha_e} \delta(\alpha)[(R_o(\alpha) + r) - R_{ec}(\alpha)]d\alpha \quad (3)$$

where,

$$\delta(\alpha) = 1 \quad \text{for } R_o(\alpha) + r > R_{ec}(\alpha) \quad (4a)$$

165  $\delta(\alpha) = 0 \quad \text{for } R_o(\alpha) + r < R_{ec}(\alpha) \quad (4b)$

If the shoreline is not well fitted into a circle, as in the example of Fig. 1, after finding the curve that best fits the shoreline, it is appropriate to set the fitting curve as EOSL and  $r$  in the direction perpendicular to the shoreline.

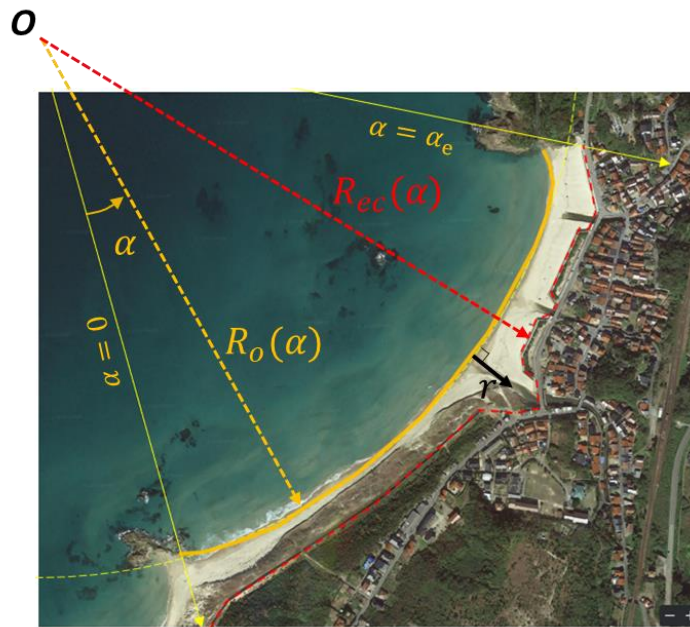


Figure 1: Conceptual diagram of combined potential erosion risk (CPER) curve (Image courtesy of Google Earth).

170

Next, the total beach erosion width  $W_t$  is calculated from the sum of all PEWs obtained from the method described above, so that

$$W_t = W_b + W_r + W_e \quad (5)$$

The right-hand-side of Eq. (5) includes the effects of (1) background erosion resulting from decrease in sediment budget due to watershed development, sand dredging, or extraction, (2) alongshore sediment redistribution and shoreline reshaping due to harbor construction, and (3) short-term erosion due to episodic storm, respectively. Because beach recovers after storm wanes,

175

the recoverable episodic erosion ( $W_e$ ) has different values depending on its recurrent interval. When  $W_t$  is calculated, as shown in Fig. 2, the overall erosion consequence  $C_t$  can be obtained from a **Combined Potential Erosion Risk curve (CPERC)**, which represent the accumulated area likely to be damaged from the EOSL.

180

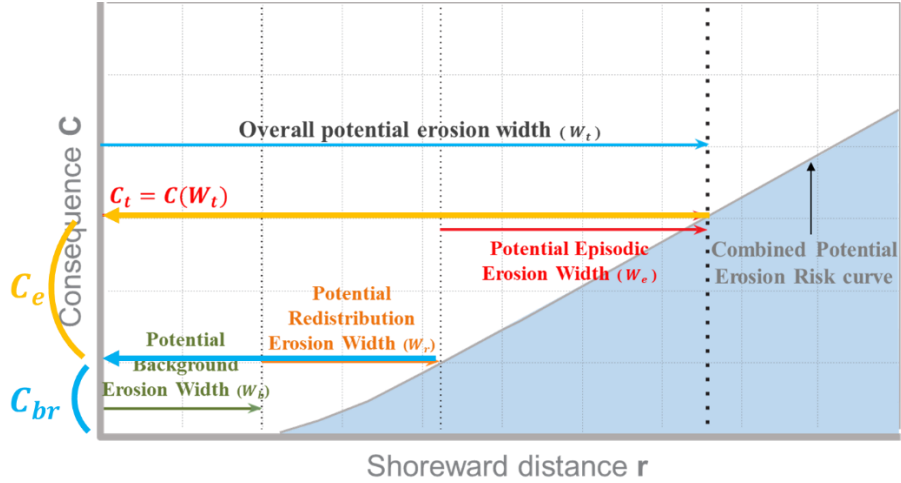


Figure 2: A combined potential erosion risk curve (CPERC) constructed from three components of potential erosion width and area.

185 The abscissa  $r$  in Fig. 2 is the shoreward distance from the average shoreline (EOSL). If the combined potential shoreline retreat  $W_t$  in Eq. (5) is substituted by  $r$ , the CPERC can also represent an area corresponds to a consequence  $C$  in Eq. (1). To calculate the CPERC area, the frequency related to the background PBEA and PREA can be regarded as one per year ( $F_{br} = 1/yr$ ), while that for the PEEA ( $F_e$ ) depends on the frequency of storm occurrence. Therefore, the combined risk  $R$  in Eq. (1) can be expressed by,

190

$$R = C_{br}F_{br} + C_e(r)F_e(r) \quad (6)$$

where  $C_{br} = C(W_b + W_r)$  and  $C_e = C(W_t) - C_{br}$ , as illustrated graphically in Fig. 2.

### 3. Assessment of Erosion Risk for Contributing Components

#### 3.1 Sediment reduction from updrift river

195

The PBEA ( $A_b$ ) accounts for the beach erosion caused by a decrease in sediment supply from river. For a sandy beach within a littoral cell (Lee and Lee, 2020), the law of mass conservation gives

$$\frac{dV}{dt} = Q_{in} - Q_{out} \quad (7)$$

where  $Q_{in}$  is the rate of sediment discharged from river (a point source), and  $Q_{out}$  is the rate of sediment leaving the cell (a sediment sink alongshore and offshore) due to wave action. The latter is constant due to continuous wave action. If  $Q_{in} < Q_{out}$  and the difference ( $\Delta Q_p = Q_{in} - Q_{out}$ ) is expressed as the product of a sediment loss constant  $K$ , then the change in beach sediment volume  $V$  (Lee and Lee, 2020) can be given by,

$$\frac{dV}{dt} = \Delta Q_p - KV \quad (8)$$

When the amount of sediment in a littoral cell is in equilibrium, the sediment loss constant  $K$  can be estimated as  $\Delta Q_p/V$ . Here, volume  $V$  in the active beach can be approximated as the product of the vertical height of the littoral zone  $D_s$  and beach surface area  $A$ . Assuming  $D_s$ , the sum of berm height and closure depth, is constant along a beach, Eq. (8) becomes

$$\frac{dA}{dt} = \frac{1}{D_s} \Delta Q_p - KA \quad (9)$$

Many studies have been performed to determine the berm height and closure depth  $D_s$  (Rosati, 2005; Cappucci et al., 2011; Cappucci et al., 2020; Pranzini et al., 2020). Although closure depth varies with wave climate and sediment particle size (Hallermeier, 1981), judging from observed beach profile data, its value has been shown to remain reasonably constant over several decades.

Since the purpose of this study is to obtain PBEA, Eq. (9) gives beach surface area  $A$  for a steady state ( $dA/dt = 0$ ) as,

$$A = \frac{\Delta Q_p}{KD_s} \quad (10)$$

where  $K$  and  $D_s$  are coefficients representing the characteristics of a beach. Therefore, if  $\Delta Q_p$  changes within a coastal environment where  $K$  and  $D_s$  are constant, the beach surface area will change accordingly. When  $\Delta Q_p$  before coastal zone development is set as  $\Delta Q_p^o$ , and if  $\Delta Q_p$  is reduced by  $\alpha \Delta Q_p^o$ , then PBEA ( $A_b$ ) can be expressed as a function of  $\alpha$  as,

$$A_b = \frac{\alpha}{KD_s} \Delta Q_p^o = \alpha A^o \quad (11)$$

Here, superscript 'o' corresponds to the beach area before development. Once  $\alpha$  is obtained, PBEA can be calculated as described above. However, due to difficulty in directly determining the  $\alpha$  value, additional information is required, such as land uses change, forestation, water storage capacity stored by dams, and river maintenance projects in the watershed (Yang, 1974; Karim and Kennedy, 1990; Wu and Xu, 2006; Slagel and Griggs, 2008; Gunawan et al., 2018).

Assuming  $A_b$  is uniformly distributed over the entire embayment with a curved length  $L_b$ , then the PBEW ( $W_b$ ) =  $A_b/L_b$ , as shown in Fig. 3.

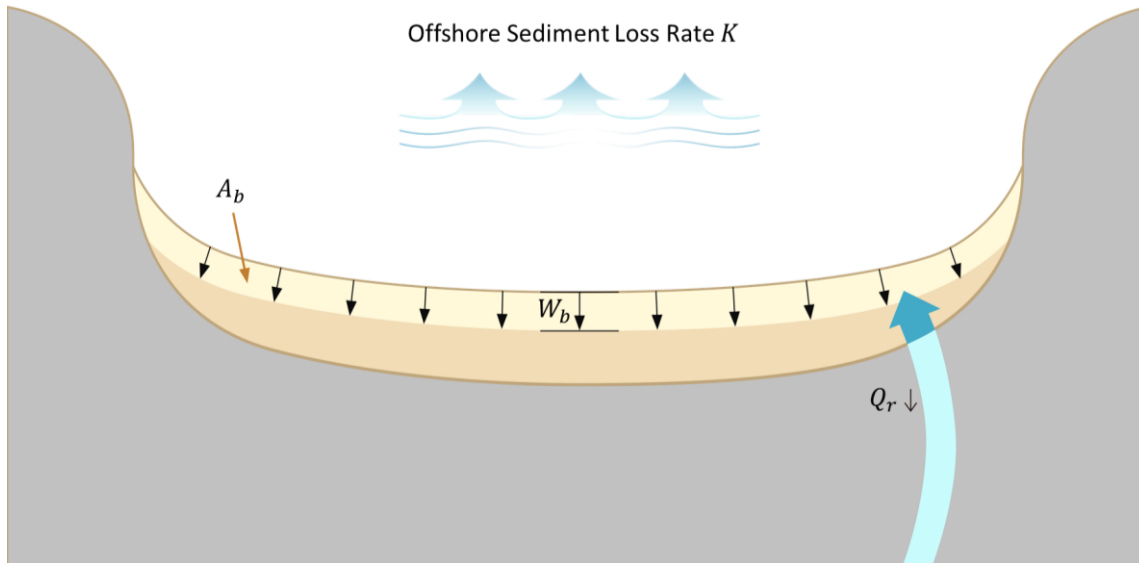


Figure 3: Conceptual diagram for the PBEA caused by sediment reduction from river.

### 3.2 Shoreline reshaping due to harbor construction

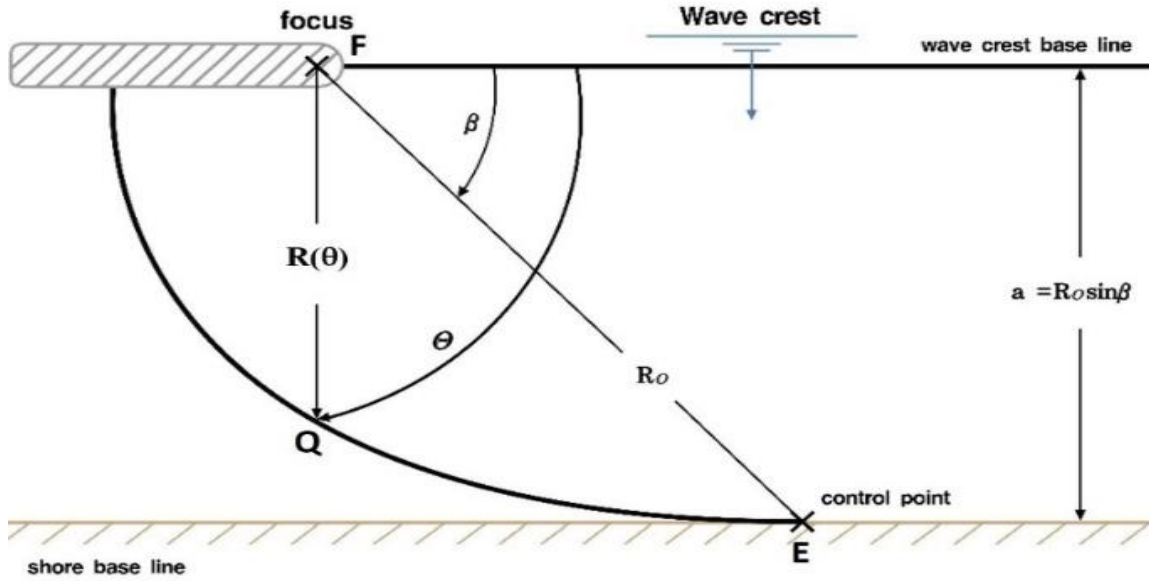
225 Harbor construction on sandy coast often changes the wave field, generating new wave diffraction and nearshore current  
 patterns. It also causes ‘shoreline reshaping’ with downdrift erosion accompanying by updrift accretion. Although the amount  
 of sediment may maintain within a cell, erosion risk area called PREA induced by the redistribution of littoral drift can be  
 assessed by an empirical shoreline model of parabolic type (i.e., PBSE; Hsu and Evans, 1989). This model can be readily  
 applied to predict the static bay shape on downdrift beach with the breakwater tip as a control point. This equation (in polar  
 230 coordinates) can be used to define two adjoining regions with a common tangent at the downdrift control point  $E$  (Fig. 4),

$$R(\theta) = \frac{a}{\sin \beta} \left[ C_0 + C_1 \left( \frac{\beta}{\theta} \right) + C_2 \left( \frac{\beta}{\theta} \right)^2 \right] \quad \text{for } \theta \geq \beta \quad (12a)$$

$$R(\theta) = \frac{a}{\sin \beta} \quad \text{for } \theta \leq \beta \quad (12b)$$

where  $R_0$  is the length of the control line ( $FE$ ) joining the parabolic focus ( $F$ ; wave diffraction point) and the downdrift control  
 point  $E$ ,  $R(\theta)$  is the radius from the focus to a point  $Q$  on the equilibrium shoreline,  $a$  is the perpendicular distance from the  
 235 wave crest baseline to point  $E$ ,  $\beta$  is the angle between the wave crest baseline and the line joining the focus and the control  
 point,  $\theta$  is the angle between the wave crest baseline and the line connecting  $F$  and  $Q$ , and  $C_0$ ,  $C_1$  and  $C_2$  are the coefficients  
 provided by Hsu and Evans (1989). An approximate expression of the PBSE is given by,

$$R(\theta) \cong \frac{\beta}{\sin \beta} \frac{a}{\theta} \quad (13)$$



240

**Figure 4: Sketch of parabolic bay shape equation and relevant geometric parameters.**

Recently, Lim et al. (2021) extend the applicability of the PBSE with polar coordinates to concave coasts. In the present case, the actual equilibrium shoreline can be estimated by shifting the downdrift segment of the predicted bay shape landward, parallel to the existing shoreline, and equating the accreted area  $A_r^+$  with the eroded area  $A_r^-$ , as shown in Fig. 5. The accreted area, which is the PREA, can also be derived from Eq. (13), rendering,

245

$$\frac{A_r}{a^2} = \frac{1}{2} [\cot \beta' + \cot \beta] + \frac{1}{2} \left( \frac{\beta}{\sin \beta} \right)^2 \left( \frac{1}{\pi - \beta'} - \frac{1}{\beta} \right) \quad (14)$$

In Eq. (14) and Fig. 5,  $\beta'$  is the angle between the focus point (i.e., the breakwater tip) and secondary breakwater. For application, Eq. (14) can be approximated as,

$$A_r \cong a^2 \left( \frac{28.8}{\beta'} - 0.004\beta \right) \quad (\beta, \beta' \text{ units: degrees}) \quad (15)$$

250

Then, the PREW  $W_r$  can be calculated from dividing the accretion area  $A_r$  by  $L_r$ , which is the length from the focus point to the farthest point on the downdrift beach or the shoreline length in the erosion section (Fig. 5).

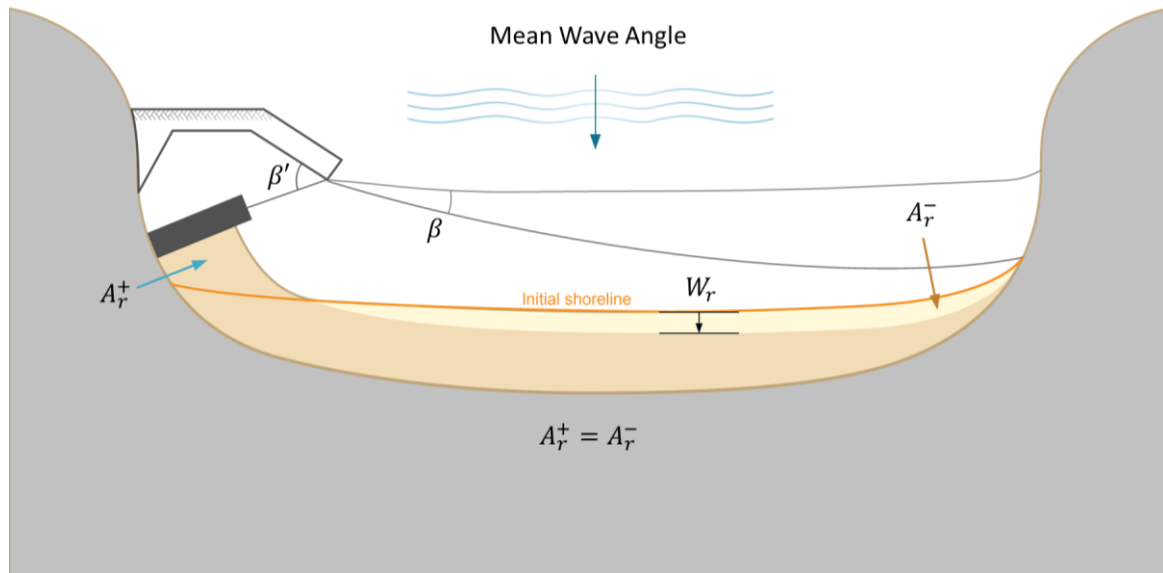


Figure 5: PREA caused by shoreline reshaping due to harbor construction.

### 3.3 Shoreline retreat due to episodic storm

The PEEA is defined as a beach surface that is temporarily eroded by storm. However, it is also an erosion characterized by a gradual return of beach profile to the original shoreline after storm wanes. Fig. 6 shows the variation of mean beach profile with a near constant depth of closure at Bongpo-Cheonjin beach. It reveals the statistical distribution of shoreline survey data performed four times in each year follows a normal distribution. Although these surveys are intended to present seasonal changes in shoreline variability, unlikely to reflect short-term changes during storm, it is confirmed that a series of survey data is sufficient for including storm effect if the sampling data of more than 8 years are multiplying by a weighting factor of 1.5 to the result of probability analysis comparing with the extreme analysis at Tairua Beach in New Zealand (Montaño et al, 2020).

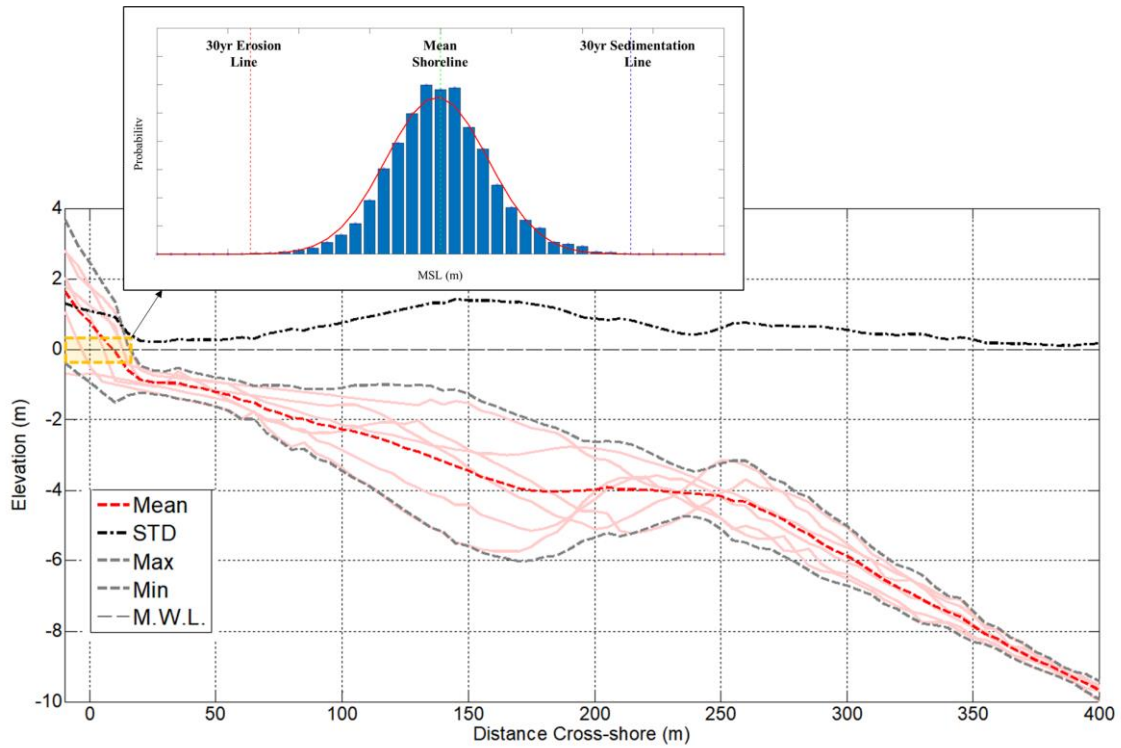


Figure 6: Variation of beach profile and shoreline position and its probability distribution (inset) at a beach in Korea.

265 When the observed shoreline data follow a normal distribution, it can be applied to assess the maximum probable erosion occurring once in  $n$  years with a probability of  $\frac{1}{4n}$  in a cumulative normal distribution curve. From which the frequency  $F$  for a shoreline variable  $x_F$  can be estimated by,

$$F(x_F) = 1 - \frac{1}{2} \left[ 1 + \operatorname{erf} \left( \frac{x_F}{\sqrt{2}} \right) \right] \quad (16)$$

From Eq. (16), the shoreline position due to episodic erosion  $S_e$  is then calculated for a shoreline variation width  $x_F$  by,

270 
$$S_e = \mu - \sigma x_F \quad (17)$$

where  $\mu$  is the mean position of shoreline and  $\sigma$  is the standard deviation of the shoreline variation width obtained from the data distribution curve. The PEEW with a certain return period can then be estimated statistically from shoreline observation data, such that

$$W_e = \sigma x_F \quad (18)$$

275 where the frequency  $F(x_F)$  corresponds to frequency  $F_e$  in the potential erosion risk given in Eq. (6). However, since the shoreline was observed four times a year, it was approximated by multiplying 1.5 to convert it into a daily statistical value of the variation. Table 1 indicates the shoreline variation  $x_{F,4}$  and the corresponding daily shoreline retreat per frequency  $F_e$ .

**Table 1: Shoreline data variation  $x_{F,4}$  and daily shoreline retreat  $x_F$  per frequency  $F_e$ .**

| Frequency $F_e$ (yr <sup>-1</sup> ) | Shoreline data variable $x_{F,4}$ (m) | Daily shoreline variable $x_F$ (m) |
|-------------------------------------|---------------------------------------|------------------------------------|
| 1                                   | 0.68                                  | 1.01                               |
| 2                                   | 1.15                                  | 1.73                               |
| 5                                   | 1.65                                  | 2.47                               |
| 10                                  | 1.96                                  | 2.94                               |
| 20                                  | 2.24                                  | 3.36                               |
| 30                                  | 2.40                                  | 3.59                               |
| 50                                  | 2.58                                  | 3.86                               |
| 70                                  | 2.69                                  | 4.04                               |
| 100                                 | 2.81                                  | 4.21                               |

280

Finally, PEEA ( $A_e$ ) is obtained by multiplying the PEEW ( $W_e$ ) with its effective shoreline length  $L_e$ . In case of the method proposed above cannot be applied because there is no shoreline survey data or the amount of data is insufficient for statistical analysis, the PEEW can be estimated using an equilibrium beach profile (Dean, 1977) from storm wave and sediment particle size data (Kim and Lee, 2018).

## 285 4. Case Study at Bongpo-Cheonjin Beach

### 4.1 Site description

The quantitative **assessment** proposed in the present study is applied to Bongpo-Cheonjin Beach (38°15'N, 128°33'E), in the northeast of Gangwon-do (province), South Korea, **where** a small Cheonjin Harbor is at its north and a large Bongpo harbor to its south (Fig. 7). **The beach is in** crenulated shape, approximately 1.1 km long, **and** is a closed littoral cell due to the existence of the breakwater (completed in November 2010) for Cheonjin Harbor at updrift and a group of natural rocks nearshore in the downdrift region. Because beach erosion had often occurred by high waves in winter, three segmented submerged breakwaters totaling 490 m in length (installed between November 2017 and November 2019) and one groin of 40 m (completed in July 2018) extended out from the rocks, eventually transformed the beach into a stable embayment (Fig. 7). Application of software MeePaSoL (Lee, 2015) developed for the PBSE (Hsu and Evans, 1989) reveals that Bongpo-Cheonjin beach is currently close to static equilibrium (using focus points B and C for the updrift and downdrift half of the beach shown in yellow curve, respectively; Fig. 7).

295

In geomorphic term, Bongpo-Cheonjin beach has received predominant waves from about N47°E direction (drawn by software MeePaSoL); whereas the prevailing wave direction in spring and summer is from N50°E and that in autumn and winter from

N30°E in the open sea. Therefore, longshore sediment transport prevails from north to south in autumn and winter, especially during high waves in winter, which had caused severe beach erosion.

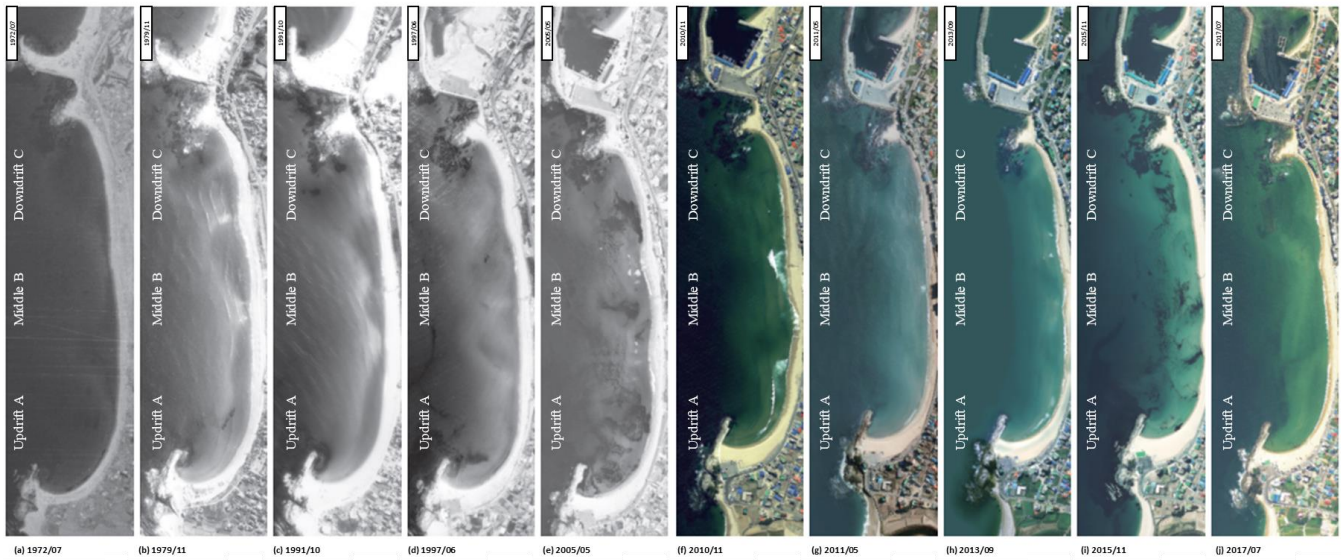


Figure 7: Aerial photograph of Bongpo-Cheonjin Beach in February 2021, showing harbors, river, shore protection structures and static bay shapes produced by software MeePaSoL on image courtesy of Google Earth.

#### 305 4.2 PBEA due to development in watershed

Cheonjin River watershed which contains three rivers and covers an area of 69.51 km<sup>2</sup> is linked to the littoral cell at Bongpo-Cheonjin Beach. Although a series of development in the watershed (e.g., construction of several small weirs, change in forest environment, and river maintenance projects) has had the potential in reducing the sediment input to the beach, its impact to the background PBEA and PBEW is found to be minimal, upon analyzing a series of 10 aerial photographs of Bongpo-Cheonjin Beach (Fig. 8) that spans over 45 years from 1972 to 2017 (i.e., in July 1972, November 1979, October 1991, June 1997, May 2005, November 2010, May 2011, September 2013, November 2015, and July 2017). Values of shoreline position, beach width and beach area are extracted from three key locations (A, B, and C marked on each sub-panels in Fig. 8) and tabulated in Table 2. In addition, 37 sets of seasonal shoreline survey data collected during 2008–2017 and NOAA's wave data are also utilized, and the results are also presented graphically in Fig. 9.

315



**Figure 8:** Aerial photographs of Bongpo-Cheonjin Beach by year: (a) 07/1972 (b) 11/1979, (c) 10/1991, (d) 06/1997, (e) 05/2005, (f) 11/2010, (g) 05/2011, (h) 09/2013, (i) 11/2015, and (j) 07/2017 on image courtesy of National Geographic Information Institute (MOF, 2018).

320 **Table 2:** Variations in beach area at three key locations of Bongpo-Cheonjin Beach marked on Fig. 8 (MOF, 2018).

| MM/YYYY | Months from previous date | Total months from 07/1972 | Updrift A (m <sup>2</sup> ) | Middle B (m <sup>2</sup> ) | Downdrift C (m <sup>2</sup> ) |
|---------|---------------------------|---------------------------|-----------------------------|----------------------------|-------------------------------|
| 07/1972 | 1                         | 1                         | 3,266                       | 12,943                     | 5,059                         |
| 11/1979 | 89                        | 90                        | 9,699                       | 15,262                     | 6,835                         |
| 10/1991 | 143                       | 233                       | 10,986                      | 14,892                     | 5,648                         |
| 06/1997 | 68                        | 301                       | 8,969                       | 13,660                     | 6,681                         |
| 05/2005 | 95                        | 396                       | 12,279                      | 14,383                     | 4,653                         |
| 11/2010 | 66                        | 462                       | 14,194                      | 15,268                     | 5,041                         |
| 05/2011 | 7                         | 469                       | 14,980                      | 15,444                     | 4,721                         |
| 09/2013 | 28                        | 497                       | 14,416                      | 13,631                     | 5,443                         |
| 11/2015 | 26                        | 523                       | 15,144                      | 15,591                     | 5,864                         |
| 07/2017 | 20                        | 543                       | 13,669                      | 9,317                      | 3,898                         |

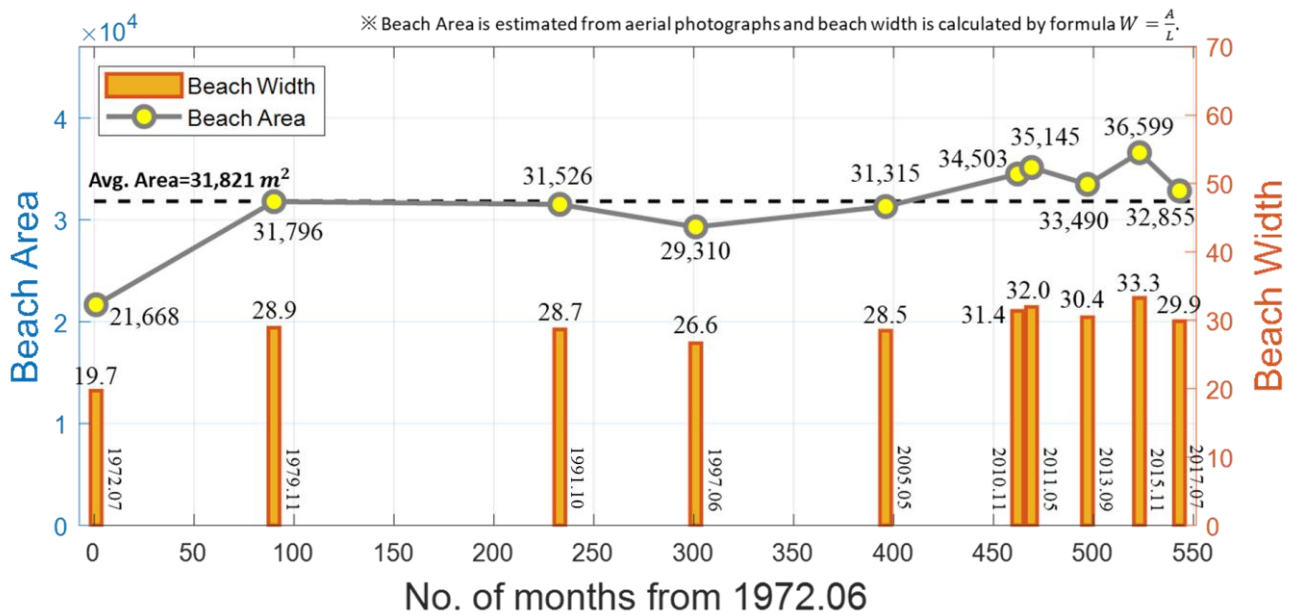


**Figure 9: Variations of beach area and width for Bongpo-Cheonjin Beach using aerial photographs.**

From each aerial photograph, the average beach width is obtained by dividing the beach area from the shoreline length at the time of photographing. Therefore, depending on the incidence wave conditions at that time, it may not be able to reflect the effect of shoreline retreat caused by cross-shore sediment transport. Nonetheless, statistical analysis indicates that the erosion width occurring at a frequency of one year is about 16.3 m at the Bongpo-Cheonjin Beach.

As shown in Fig. 9, that since 1979.11 (November), total beach area at Bongpo-Cheonjin has remained around 31,800 m<sup>2</sup>, about the average of 31,821 m<sup>2</sup>, or higher after 2005.05, except between 1991.11 and 2005.05, whereas beach width has maintained about 28 m or more, except in 1997.06 when it was reduced to 26.6 m. Although small submerged weirs were built along Cheonjin River, its effect on the background sediment budget  $A_b$  is minimal, due to the small storage capacity of the weirs. Hence, the PBEW  $W_b$  may be ignored in this study.

#### 4.3 PREA caused by the construction of harbor breakwater

Again in Fig. 9, the averaged beach width of Bongpo-Cheonjin Beach appears to be remained at about 30 m for a long time after mid 2008 (by linear interpolation between 2005.05 and 2010.11), in spite of the regional shoreline advance to form a static bay-shape after the construction of the Cheonjin Harbor breakwater. During this period of time, shoreline reshaping had resulted in sediment deposition in the vicinity of the breakwater (at updrift A) and accompanying erosion (at downdrift C) of the beach as given in Table 2.

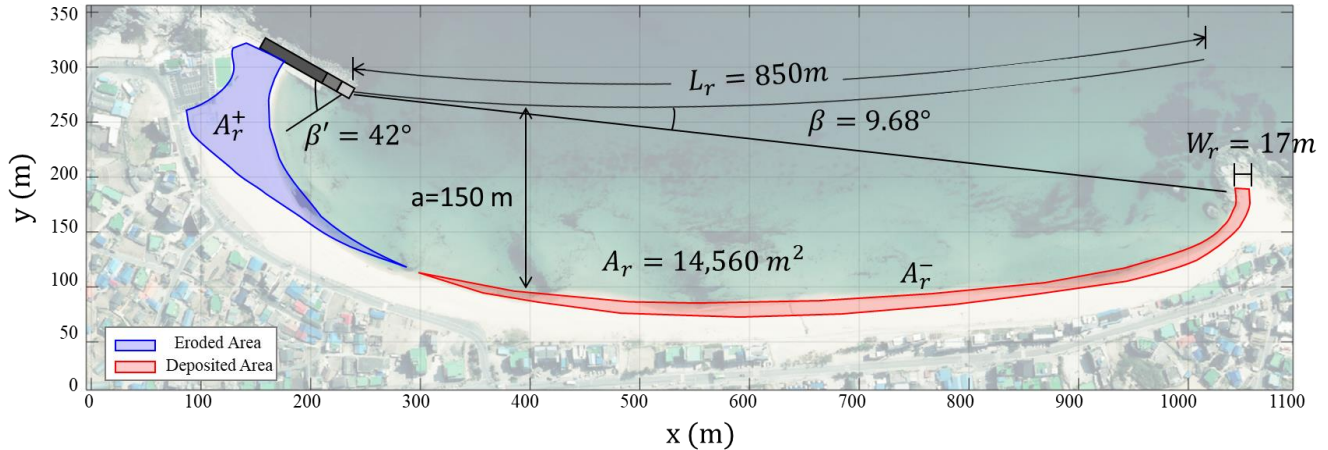
The PREA can be approximated by the bay-shape shoreline feature across the whole Bongpo-Cheonjin Beach (Fig. 10). First, the equivalent wave obliquity ( $\beta$ ) from the tip of the harbor breakwater can be approximated from the geometry of indentation ( $a$ ) in relation to the beach length ( $L_r$ ),

$$\beta = \tan^{-1}\left(\frac{a}{L_r}\right) = \tan^{-1}\left(\frac{150}{850}\right) = 9.68^\circ \quad (19)$$

The PREA  $A_r$  is then obtained by substituting the calculated  $\beta$  with  $\beta'$ , as indicated in Fig. 5 and Eq. (15),

$$\frac{A_r}{a^2} \cong \frac{28.8}{\beta'} - 0.004\beta = \frac{28.8}{42} - 0.004 \times 9.68 = 0.647 \quad (\beta \text{ and } \beta' \text{ units: degrees}) \quad (20)$$

For  $a = 150$  m (Fig. 10), Eq. (20) gives  $A_r = 14,560$  m<sup>2</sup>. The relationship between  $\beta$  and  $\beta'$  in Eq. (15) can be plotted (Fig. 11) to obtain the dimensionless PREA ( $\frac{A_r}{a^2}$ ) with values from 0 to 10. Alternatively, the value for  $A_r/a^2$  can be obtained graphically from Fig. 11. By equating  $A_r^+$  with  $A_r^-$  (Fig. 10), the amount of beach erosion width  $W_r$  is finally estimated as 17 m by inputting the beach length from the breakwater ( $L_r = 850$  m) into Eq. (2).



350

**Figure 10:** Calculation of PREA at Bongpo-Cheonjin Beach on image courtesy of National Geographic Information Institute (MOF, 2020).

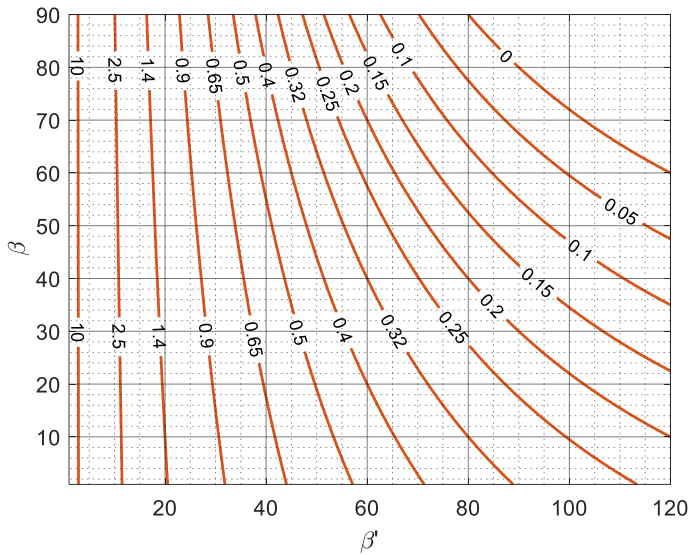


**Figure 11:** Diagram for determining dimensionless PREA ( $\frac{A_r}{a^2}$ ) ranging from 0 to 10 in Eq. (15).

#### 355 4.4 PEEA due to shoreline retreat during storm

Routine shoreline surveys have been conducted at least four times per annum for beaches in Gangwon-do, South Korea, since the 2000s. More specifically, a total of 37 sets of seasonal data were collected over 10 years from 2008 to 2017 for Bongpo-Cheonjin Beach. These data are plotted and fitted by a normal distribution (Fig. 12) to show local shoreline changes with standard deviation of  $\sigma = 5.5$  m. Fig. 12 also compares alongshore distribution of the mean shoreline and eroded shoreline of 360 30-year return period from statistical analyses ( $x_F = 3.59$ ). The beach width due to the PEEW is evaluated as the value with the range from from 5.57 m to 23.16 m ( $1 \text{ yr} \leq F_e \leq 100 \text{ yrs}$ ).

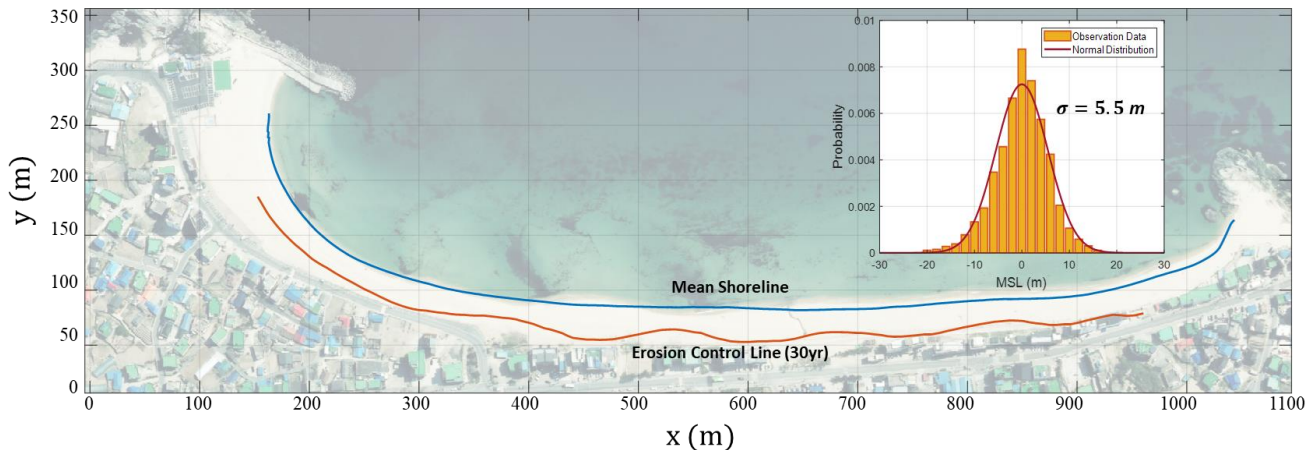


**Figure 12:** PEEA at Bongpo-Cheonjin Beach, showing standard deviation  $\sigma$  and mean encroachment  $\sigma x_F$  with 30-year return period (within inset) on image courtesy of National Geographic Information Institute (MOF, 2020).

365 **4.5 Combined potential erosion risk at Bongpo-Cheonjin Beach**

The potential erosion risk to a beach can be obtained by accumulating all the erosion risk widths from each contributing factor, resulting in a **CPER curve** (Sect. 2.3 and Fig. 2). In Fig. 13, the **CPER curve** accounts for the erosion risk distance from the average shoreline (EOSL). At Bongpo-Cheonjin Beach, the PBEW  $W_b$  and PREW  $W_r$  are estimated as 0 m and 17 m, respectively, thus representing the sum of first two individual components  $W_b + W_r = 17$  m. Furthermore, by letting the combined erosion risk width  $W_t$  (Eq. 5) at 5 m intervals, up to 50 m, the corresponding value for consequence  $C_t$  can be tabulated as in **Table 3**.

Because PEEW  $W_e$  is a function of the return period (frequency) of storm occurrence, the total shoreline retreat ( $W_t$ ), consequence ( $C_t$ ) and erosion risk ( $R$ ; Eqs. 1 and 6) are calculated for several specific return period (in years) of storm, as shown in **Table 4**. In addition, Fig. 13 illustrates the consequence  $C_t$  per return period  $T_r$  ( $1/F_e$ ), which are obtained using the **CPER curve**, while Fig. 14 shows the variation of consequence and the combined potential erosion risk with respect to storm return period at Bongpo-Cheonjin Beach.

**Table 3: Relationship between combined shoreline retreat  $W_t$  and consequence  $C_t$  for Bongpo-Cheonjin Beach.**

|                         |   |    |    |    |     |       |       |       |        |        |
|-------------------------|---|----|----|----|-----|-------|-------|-------|--------|--------|
| $r = W_t$ (m)           | 5 | 10 | 15 | 20 | 25  | 30    | 35    | 40    | 45     | 50     |
| $C_t$ (m <sup>2</sup> ) | 0 | 0  | 0  | 0  | 181 | 1,545 | 3,997 | 6,951 | 10,299 | 13,989 |

380 **Table 4: Potential erosion risk per return period  $T_r$  for Bongpo-Cheonjin Beach using CPER curve.**

| Return period $T_r$ (yr) | Shoreline retreat $W_t$ ( $W_e$ ) (m) | Consequence $C_t$ (m <sup>2</sup> ) | Potential risk $R$ (m <sup>2</sup> ) |
|--------------------------|---------------------------------------|-------------------------------------|--------------------------------------|
| 1                        | 22.57 (5.57)                          | 20.9                                | 20.9                                 |
| 2                        | 26.49 (9.49)                          | 446.9                               | 223.5                                |
| 5                        | 30.57 (13.57)                         | 1787.7                              | 357.5                                |
| 10                       | 33.17 (16.17)                         | 3034.0                              | 303.4                                |
| 20                       | 35.49 (18.49)                         | 4263.5                              | 213.2                                |
| 30                       | 36.75 (19.75)                         | 4969.4                              | 165.6                                |
| 50                       | 38.25 (21.25)                         | 5861.5                              | 117.2                                |
| 70                       | 39.19 (22.19)                         | 6440.7                              | 92.0                                 |
| 100                      | 40.16 (23.16)                         | 7052.6                              | 70.5                                 |

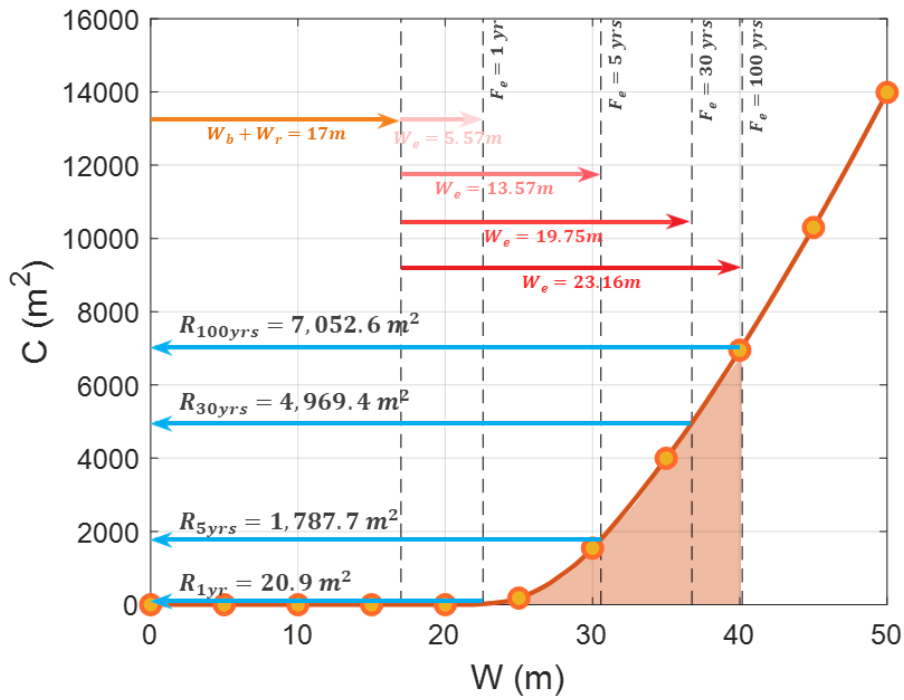


**Figure 13:** Estimation of combined potential erosion risk using the CPER curve for Bongpo-Cheonjin Beach.

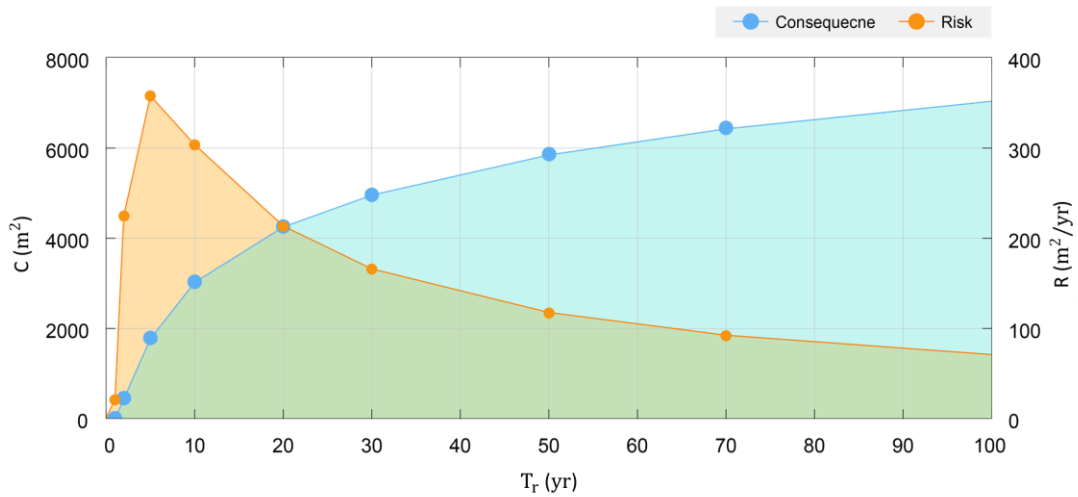


**Figure 14:** Consequence  $C$  and potential risk  $R$  with respect to  $T_r$  at Bongpo-Cheonjin Beach.

Overall, from the analysis of potential beach erosion area and width for the three key factors at Bongpo-Cheonjin Beach, the PBEW may be considered as insignificant, hence  $W_b \approx 0$ , while PREW ( $W_r$ ) is estimated as 17 m following a 40-m extension to the breakwater for Cheonjin harbor. In addition, the PEEW ( $W_e$ ) value is estimated to be between 5.57 m and 19.75 m for the storm return period ( $F_e$ ) of 1 and 30 years, respectively. Upon applying the combined shoreline retreat ( $W_b + W_r + W_e$ ) to the CPER curve, it yields the total eroded beach area ranging from 20.9 m<sup>2</sup> to 4969.4 m<sup>2</sup> (see Fig. 13 and Table 4). For a storm in 30-year return period, this implies that a beach area totalling 4,969.4 m<sup>2</sup> (or beach width about 36.75 m) might be eroded once in every 30 years, thus requiring appropriate engineering solutions (such as coastal setback, beach nourishment or others) to conserve the coastal environment at Bongpo-Cheonjin Beach.

## 5. Discussions

Limitations of the assessment method proposed in this study are briefly described, together with additional considerations, to enhance the applicability of this methodology to different coastal environments.

- (1) Although the purpose of this study is to apply an assessment method to Bongpo-Cheonjin Beach, which is a shallow embayment or a semi-closed coastal cell, the method proposed is not limited to headland-bay beaches. It is also applicable to open beaches with suitable modification to the mechanisms examined in this study.
- (2) The proposed *combined potential erosion risk curve* (CPERC) includes individual risk component assessed for background sediment from a river at updrift, a fishing harbor with breakwater extension and storm waves in winter. The construction of CPERC is based on a simple arithmetic sum to represent the case of worse scenario, rather by a multivariable regression analysis. It cannot predict the temporal change of erosion risk. To improve the reliability of this method, the temporal beach change and the scale of each contributing factor versus time must be examined, especially from that induced by the episodic storm which occurs only sporadically, whereas the other two are either almost constant or increasing gradually.
- (3) For Bongpo-Cheonjin Beach, the potential background erosion width (PBEW,  $W_b$ ) is negligible, indicating the variation of sediment supply from the watershed is minimal. However, after large dam is constructed within a watershed, the time-dependent change in the beach width must be considered. Theoretical solution given by Lee and Lee (2020) suggests the effects of the sand loss rate  $K_b$  into the open sea and the decrease rate  $\alpha$  of sediment supply to the beach can be expressed as
$$W_b(t) = \alpha W^o [1 - \exp(-K_b t)] \quad (21)$$
where  $\alpha$  and  $K_b$  are constant, and the corresponding beach area is assumed to converge to  $(1 - \alpha)A^o$ , in which  $A^o$  is the initial area. Eq. (21) shows that the beach area decreases rapidly at the beginning, but converges to 95% or more of the equilibrium state when  $t$  is greater than  $3/K_b$  years.
- (4) To increase the accuracy of potential erosion width (PREW,  $W_r$ ) due to shoreline reshaping caused by breakwater construction for harbor, empirical formula (e.g., CERC equation in Shore Protection Manual, 1984) can be applied.

420 Starting from the angle difference between the initial and equilibrium shoreline angles at the boundary of erosion and deposition, the temporal width change is obtained by applying an exponentially converging angle change to the formula for longshore sediment transport.

$$W_r(t) = W_r^u [1 - \exp(-K_r t)] \quad (22)$$

where  $W_r^u$  is the ultimate beach width due to longshore sediment transport,  $K_r$  is the rate of change of angle according to the time at the junction, which is estimated by dividing the beach length  $L_r$  and the vertical littoral height  $D_s$  in the formula for longshore sediment transport. The equilibrium shoreline angle due to harbor or coastal structures can be obtained based on the PBSE of Hsu and Evans (1989).

425 (5) For potential beach erosion due episodic storm (PEEW,  $W_e$ ) that can be recovered after storm wanes, Yates et al. (2009) have confirmed that a linear relationship exists between the location of the shoreline and swell wave energy in field observation. Applying this recoverable process, the shoreline change model proposed by Miller and Dean (2004) can be expressed by an ODE equation (Kim, 2021),

$$\frac{dW_e}{dt} = K_e \left( \frac{E_b}{a} - W_e \right) \quad (23)$$

where  $K_e$  is a beach recovery factor,  $E_b$  is the wave energy at the breaking point, and  $a$  is a beach response factor between wave energy  $E_b$  and the mean shoreline. When the value of  $K_e$ , which is unique for each beach, is known, the temporal change of shoreline can be estimated from Eq. (23) for given wave energy. Alternatively, SBEACH model may be used (Larson and Kraus, 1989; Larsson et al., 1990).

## 5. Concluding Remarks

This study presents a quantitative method for assessing the potential erosion area (PEA) and potential erosion width (PEW) due to development in watershed, harbor construction, and storm impact. Aerial photographs, beach survey and NOAA's wave data are applied to support the analysis, while omitting sea-level rise. The results are used to produce a combined potential erosion risk curve (CPERC) for planning coastal protection or restoration projects, which includes the effective of potential risk induced by storm in different return period of occurrence. For example, the potential erosion risk due to storm (PEEW,  $W_e$ ) in 30-year return period is estimated about 19.75 m (Table 4) that gives the total potential erosion risk width ( $W_t$ ) of 36.75 m, which is greater than the beach width of 30 m from the current averaged shoreline (EOSL), thus calling engineering solution to protect the Bongpo-Cheonjin Beach. Due to the potential severity of predicted beach erosion risk, beach nourishment with three submerged detached breakwaters (each 160 m long with gap 70 m) have been constructed during November 2017 to November 2019, with a short groin (40 m) completed in July 2018 (Fig. 7). These have satisfactorily transformed Bongpo-Cheonjin Beach into a stable embayment since the completion of the engineering work.

450 Upon applying the risk assessment method presented in this paper, it is possible to determine the optimal strategy, comparing the total cost of risk to the eroding section with the average annual cost of erosion protection. Moreover, the proposed methodology is helpful not only for assessing beach erosion risk quantitatively but also for devising engineering countermeasures to mitigate the causes of erosion. Further research is recommended in applying the methodology described in this paper to beaches suffering severe erosion, so that this method can be improved and benefit other coastal communities from applying this method.

455 **Data availability**

Not applicable.

**Author contributions**

Supervision, J.L.L.; Writing—original draft, C.L.; Writing—review & editing, C.L., T.K., S.L. Y.J.Y. and J.L.L.; Data acquisition, C.L., T.K. and S.L.. All authors have read and agreed to the published version of the manuscript.

460 **Competing interests**

The authors declare no conflicts of interest.

**Acknowledgements**

This research is part of a project entitled 'Practical Technologies for Coastal Erosion Control and Countermeasure' supported by the Ministry of Oceans and Fisheries, Korea.

465

**References**

- Ab Razak, M. S., Jamaluddin, N. and Mohd Nor, N. A. Z.: The platform stability of embayed beaches on the west coast of Peninsular Malaysia, JESTEC, 80, 33-42, 2018a.
- 470 Ab Razak, M. S., Mohd Nor, N. A. Z. and Jamaluddin, N.: Platform stability of embayed beaches on the east coast of Peninsular Malaysia, JESTEC, 13, 435-448, 2018b.

- Anh, D. T. K., Stive, M. J. F., Brouwer, R. L. and de Vries, S.: Analysis of embayed beach platform stability in Danang, Vietnam, Proceedings of the 36th IAHR World Congress, The Hague, The Netherlands, 6-28, June-3 July 2015.
- 475 Ballesteros, C., Jiménez, J. A., Valdemoro, H. I., and Bosom, E.: Erosion consequences on beach functions along the Maresme coast (NW Mediterranean, Spain), *Natural Hazards*, 90(1), 173-195, 2018.
- Bayram, A., Larson, M. and Hanson, H.: A new formula for the total longshore sediment transport rate, *Coastal Eng.*, 54, 700–710, 2007.
- 480 Beven II, J. L., Avila, L. A., Blake, E. S., Brown, D. P., Franklin, J. L., Knabb, R. D., Pasch, R. J., Rhome, J. R., and Stewart, S. R.: Atlantic Hurricane Season of 2005, *Mon. Weather Rev.*, 136, 1109–1173, <https://doi.org/10.1175/2007MWR2074.1>, 2008.
- Bowman, D., Guillén, J., López, L. and Pellegrino, V.: Planview geometry and morphological characteristics of pocket beaches on the Catalan coast (Spain), *Geomorphology*, 108, 191–199, 2009.
- Bray, M. J., Carter, D. J. and Hooke, J. M.: Littoral cell definition and budgets for central southern England, *J. Coastal Res.*, 11(2), 381-400, 1995.
- 485 Callaghan, D. P., Ranasinghe, R., Nielsen, P., Larson, M., Short, A. D.: Process-determined coastal erosion hazards, Proceedings of the 31st International Conference on Coastal Engineering, World Scientific, 4227–4236, 2008.
- Casas-Prat, M., Sierra, J. P.: Trend analysis of wave direction and associated impacts on the Catalan coast, *Climatic Change*, 115, 667–691, <https://doi.org/10.1007/s10584-012-0466-9>, 2012.
- CERC (Coastal Engineering Research Center): Shore Protection Manual, 4th Ed. U.S. Army Corps of Engineers, Waterways Experiment Station, Coastal Engineering Research Center, U.S. Government Printing Office, Washington, D.C., 1984.
- 490 Cooper, N. J.: Engineering Performance and Geomorphic Impacts of Shoreline Management at Contrasting Sites in Southern England, Ph.D. Thesis, University of Portsmouth, Hampshire, England, 1997.
- Cooper, N. J. and Pethick, J. S.: Sediment budget approach to addressing coastal erosion problems in St. Queen’s Bay, Jersey, Channel Island, *J. Coast. Res.*, 21, 112–122, 2005. [CrossRef]
- 495 Dean, R. G.: Equilibrium beach profiles: U.S. Atlantic and Gulf Coasts, Technical Report, No. 12, Department of Civil Engineering, University of Delaware, 1977.
- Dolan, T. J., Castens, P. G., Sonu, C. J. and Egense, A. K.: Review of sediment budget methodology: ocean side littoral cell, California, Proceedings of Coastal Sediments ’87, ASCE, 1289-1304, 1987.
- Hubbard, D. W.: *The Failure of Management: Why It’s Broken and How to Fix It*, John Wiley & Sons, Hoboken, 2009.
- 500 Edward, B. T., Abby, S., Juan, C. S., Laura, E., Timothy, M. and Rost, P.: Sand mining impacts on long-term dune erosion in southern Monterey Bay, *Marine Geology*, 229, 1-2, 45-58, 2006.
- Foley, M. M., Jonathan, A. W., Andrew, R., Andrew, W. S., Patrick, B. S., Jeffrey, J. D., Matthew, M. B., Rebecca, P., Guy, G. and Randal, M.: Coastal habitat and biological community response to dam removal on the Elwha River, *Ecol. Monogr.*, 87, 552-577, 2017.

- 505 González, M., Medina, R. and Losada, M. A.: On the design of beach nourishment projects using static equilibrium concepts: Application to Spanish coast, *Coast. Eng.*, 57 (2), 227-240, 2010.
- Hansson, S. O.: Risk, *The Stanford Encyclopedia of Philosophy* (Summer 2007 Edition), Edward N. Zalta (ed.), 2007.
- Harley, M., Armaroli, C., and Ciavola, P.: Evaluation of XBeach predictions for a real-time warning system in Emilia-Romagna, Northern Italy, *J. Coast. Res.*, 64, 1861–1865, 2011.
- 510 Herrington, S. P., Li, B. and Brooks, S.: Static equilibrium bays in coast protection, Marine Engineering Group, Institution of Civil Engineers: London, UK, 2007.
- Hsu, J. R. C. and Evans, C.: Parabolic bay shapes and applications, *Proceedings of Institution of Civil Engineers, Part 2, Vol. 87*, Thomas Telford, London, 557-570, 1989.
- Inman, D. L. and Jenkins, S. A.: The Nile littoral cell and man's impact on the coastal zone of the southeastern Mediterranean, Coastal Eng. Proceedings, 1, 19, 109, 1984.
- 515 Kamphuis, J. W.: Alongshore transport of sand, *Proceedings of the 28th International Conference on Coastal Engineering, ASCE*, 2478-2490, 2002.
- Kana, T. and Stevens, F.: Coastal geomorphology and sand budgets applied to beach nourishment, *Proceedings of the Coastal Engineering Practice '92*, ASCE, 29–44, 1992.
- 520 Kaplan, S., and Garrick, B. J.: On the quantitative definition of risk, *Risk Analysis*, 1, 11–27, 1981.
- Kim, T. K.: The Duration-Limited Shoreline Response under a Storm Wave Incidence by the Concept of Horizontal Behavior of Suspended Sediments, Ph.D. Thesis, University of Sungkyunkwan, Suwon, South Korea, 2021.
- Kim, T. K. and Lee, J. L.: Analysis of shoreline response due to wave energy incidence using an equilibrium beach profile concept, *J. Ocean Eng. Technol.*, 2(1), 55–65, 2018.
- 525 Knight, F. H.: *Risk, Uncertainty and Profit*, Chicago, Houghton Mifflin Company, 1921.
- Komar, P. D. and Inman D. L.: Longshore and transport on beaches, *J. Geophys. Res.*, 75, 5914–5927, 1970.
- Kunz, M., Mühr, B., Kunz-Plapp, T., Daniell, J. E., Khazai, B., Wenzel, F., Vannieuwenhuyse, M., Comes, T., Elmer, F., Schröter, K., Fohringer, J., Münzberg, T., Lucas, C., and Zschau, J.: Investigation of superstorm Sandy 2012 in a multidisciplinary approach, *Nat. Hazards Earth Syst. Sci.*, 13, 2579–2598, <https://doi.org/10.5194/nhess-13-2579-2013>, 2013.
- 530 Larson, M. and Kraus, N.C.: SBEACH: Numerical model for simulating storm-induced beach change, Report 1, Empirical foundation and model development, Tech. Report CERC-89-9, Coastal Engineering Research Center, US Army Corps of Engineers, Washington DC, USA, 1989.
- Larson, M., Kraus, N.C. and Byrnes, M.R.: Numerical model for simulating storm-induced beach change, Report 2, Numerical formulation and model tests, Tech. Report CERC-89-9, Coastal Engineering Research Center, US Army Corps of Engineers, Washington DC, USA, 1990.
- 535 Lee, J. L.: MeePaSoL: MATLAB-GUI based software package, Sungkyunkwan University, SKKU Copyright No. C-2015-02461, 2015.

- Lee, S. and Lee, J. L.: Estimation of background erosion rate at Janghang Beach due to the construction of Geum estuary tidal barrier in Korea, *J. Mar. Sci. Eng.*, 8, 551, 2020.
- 540
- Lim, C., Lee, J. and Lee, J. L.: Simulation of bay-shaped shorelines after the construction of large-scale structures by using a parabolic bay shape equation, *J. Mar. Sci. Eng.*, 9, 43, 2021.
- McCall, R. T., Van Thiel de Vries, J. S. M., Plant, N. G., Van Dongeren, A. R., Roelvink, J. A., Thompson, D. M., and Reniers, A. J. H. M.: Two-dimensional time dependent hurricane overwash and erosion modeling at Santa Rosa Island, *Coast. Eng.*, 57, 668–683, <https://doi.org/10.1016/j.coastaleng.2010.02.006>, 2010.
- 545
- Miller, J. K. and Dean, R. G.: A simple new shoreline change model, *Coastal Eng.*, 51 (7), 531–556, 2004.
- Ministry of Oceans and Fisheries (MOF): Development of Coastal Erosion Control Technology, Ministry of Oceans and Fisheries R&D Report, 2020.
- Ministry of Oceans and Fisheries (MOF): Research on the Actual Conditions of Coastal Erosion, Ministry of Oceans and Fisheries R&D Report, 2018.
- 550
- Montaño, J., Coco, G., Antolínez, J. A. A., Beuzen, T., Bryan, K. R. Cagigal, L. Castelle, B., Davidson, M. A., Goldstein, E. B., Ibaceta, R., Idier, D., Ludka, B. C., Masoud-Ansari, S., Méndez, F. J., Murray, A. B., Plant, N. G., Ratliff, K. M., Robinet, A., Rueda, A., Sénéchal, N., Simmons, J. A., Splinter, K. D., Stephens, S., Townend, I., Vitousek, S., and Vos, K.: Blind Testing of Shoreline Evolution Models, *Scientific Reports*, 10, 2137, 2020.
- 555
- Pelnard-Considere, R.: Essai de théorie de l'évolution des forms de rivages en plages de sable et de galets, *Quatrième Journées de L'hydraulique*, Paris, 4, 289–298, 1957.
- Pethick, J. S.: Geomorphological Assessment Draft Report to Environment Committee, Environment Committee, St. Queen's Bay, **JE**, USA, 1996.
- Rasmussen, N.C.: Reactor safety study. An assessment of accident risks in U. S. commercial nuclear power plants, Executive summary: main report. [PWR and BWR], USA, doi:10.2172/7134131, 1975.
- 560
- Roelvink, D. and Reniers, A.: *Advances in Coastal and Ocean Engineering, Vol. 12, A Guide to Modeling Coastal Morphology*, 2012.
- Roelvink, D., Reniers, A., van Dongeren, A., van Thiel de Vries, J., McCall, R., and Lescinski, J.: Modelling storm impacts on beaches, dunes and barrier islands, *Coast. Eng.*, 56, 1133–1152, <https://doi.org/10.1016/j.coastaleng.2009.08.006>, 2009.
- 565
- Sanuy, M., Duo, E., Jäger, W. S., Ciavola, P. and Jiménez, J. A.: Linking source with consequences of coastal storm impacts for climate change and risk reduction scenarios for Mediterranean sandy beaches, *Nat. Hazards Earth Syst. Sci.*, 18, 1825–1847, <https://doi.org/10.5194/nhess-18-1825-2018>, 2018.
- Silveira, L. F., Klein, A. H. F. and Tessler, M. G.: Headland-bay beach platform stability of Santa Catarina State and the northern coast of São Paulo State, **Brazil**, *J. Oceanogr.*, 58, 101–122, 2010.
- 570
- Stive, M. J. F., Aarninkhof, S. G. J., Hamm, L., Hanson, H., Larson, M., Wijnberg, K. M., Nicholls, R. J., Capobianco, M.: Variability of shore and shoreline evolution, *Coast Eng.*, 47, 211–235, 2002.

- Stive, M. J. F., Ranasinghe, R., Cowell, P.: Sea level rise and coastal erosion. In: Kim, Y. (Ed.), *Handbook of Coastal and Ocean Engineering*, World Scientific, 1023–1038, 2009.
- 575 Spencer, T., Brooks, S. M., Evans, B. R., Tempest, J. A., and Möller, I.: Southern North Sea storm surge event of 5 December 2013: Water levels, waves and coastal impacts, *Earth-Sci. Rev.*, 146, 120–145, <https://doi.org/10.1016/j.earscirev.2015.04.002>, 2015.
- Swart, D. H.: *Offshore sediment transport and equilibrium beach profiles*, Tech. Rep. Publ. 131, Delft Hydraulics Lab, Delft, Netherlands, 1974.
- 580 Thomas, T., Williams, A. T., Rangel-Buitrago, N., Phillips, M. and Anfuso, G.: Assessing embayment equilibrium state, beach rotation and environmental forcing influences, Tenby Southern Wales, UK., *J. Mar. Sci. Eng.*, 4, 30, 2016.
- Toimil, A., Losada, I. J., Camus, P., and Díaz-Simal, P.: Managing coastal erosion under climate change at the regional scale, *Coastal Eng.*, 128, 106-122, 2017.
- USACE: *Coastal Engineering Manual* (online). US Army Corps of Engineers, Washington, D.C., 2002.
- 585 Van Verseveld, H. C. W., Van Dongeren, A. R., Plant, N. G., Jäger, W. S., and den Heijer, C.: Modelling multi-hazard hurricane damages on an urbanized coast with a Bayesian Network approach, *Coast. Eng.*, 103, 1–14, <https://doi.org/10.1016/j.coastaleng.2015.05.006>, 2015.
- Wainwright, D. J., Ranasinghe, R., Callaghan, D. P., Woodroffe, C. D., Jongejan, R., Dougherty, A. J., Rogers, K., Cowell, P. J.: Moving from deterministic towards probabilistic coastal hazard and risk assessment: development of a modelling framework and application to Narrabeen Beach, New South Wales, Australia, *Coast Eng.*, 96, 92–99, 2015.
- 590 Wang, H., Dalrymple, R. A., and Shiau, J. C.: Computer simulation of beach erosion and profile modification due to waves, *Proc. 2nd Annual Symp. Waterways, Harbours and Coastal Engng. Div. ASCE on Modeling Techniques (Modeling '75: San Franc)*, 2, 1369-1384, 1975.
- Warrick, J. A., Stevens, A. W., Miller, I. M., Harrison, S. R., Ritchie, A. C., and Gelfenbaum, G.: World's largest dam removal reverses coastal erosion, *Sci. Rep.*, 1–12, 2019.
- 595 Wright, L. D., Short, A. D. and Green, M. O.: Short-term changes in the morphologic states of beaches and surf zones: an empirical model, *Mar. Geol.*, 62: 339-364, 1985.
- Yates, M. L., Guza, R. T. and O'Reilly, W. C.: Equilibrium shoreline response: observations and modeling, *Journal of Geophysical Research*, 114(C9), C09014, 2009.
- Yu, J. T. and Chen, Z. S.: Study on headland-bay sandy cast stability in South China coasts, *China Ocean Eng.*, 25, 1, 2011.
- 600 Zacharioudaki, A. and Reeve, D. E.: Shoreline evolution under climate change wave scenarios, *Climate Change*, 108, 73–105. <http://dx.doi.org/10.1007/s10584-010-0011-7>, 2011.